Journal Name

COMMUNICATION

Hidden Aryl-Exchange Processes in Stable 16e Rh^{III} [RhCp*Ar$_2$] Complexes, and their Unexpected Transmetalation Mechanism†

M. N. Peñas-Defrutos,[a] C. Bartolomé,*[a] M. García-Melchor*[b] and P. Espinet*[a]

Experiments mixing the stable 16e 5-coordinate complexes [RhCp*Ar$_2$] (Cp* = C$_5$Me$_5$; Ar = C$_6$F$_5$, C$_6$F$_3$Cl$_2$-3,5) uncover fast aryl transmetalations. Unexpectedly, as supported computationally, these exchanges are not spontaneous, but catalyzed by minute amounts of 18e (μ-OH)$_2$[RhCp*Ar]$_2$ as a source of 16e [RhCp*Ar(OH)]. The OH group is an amazingly efficient bridging partner to diminish the activation barrier of transmetalation.

The reactivity of eighteen-electron octahedral organometallic complexes is assumed to start with a one-ligand dissociation to give sixteen-electron electrophilic species. This is textbook knowledge based on classical ligand-substitution studies of coordination compounds. However, modern mechanistic studies of other reactions on organometallic complexes are scarce.[1] M^{III}Cp* (Cp* = C$_5$Me$_5$; M = Rh, Ir) continue to attract attention for their reactivity and properties. For instance, Rh^{III}Cp* (Cp* = C$_5$Me$_5$) complexes have been reported very recently to catalyse dehydrogenative coupling formation of bis-heteroarylated phenols via a 5-coordinate 16e complex.[2] In a different line, Ir^{III}Cp* complexes with aryl groups have been studied in water oxidation catalysis.[3] Here we report the synthesis of unusually stable 16e complexes [RhCp*Ar$_2$] (Ar = C$_6$F$_5$ = Pf, or C$_6$F$_3$Cl$_2$-3,5 = Rf), as models of intermediates formed from octahedral complexes after ligand dissociation, and discuss their structures, and dynamic processes relevant to their reactivity.

The transmetalation reaction of *anti*-(μ-Cl)$_2$[RhCp*Cl]$_2$ (**1**)[4,5] with excess AgAr·n(NCMe)[6] (Ar = Rf, Pf)[7] affords complexes [RhCp*Rf$_2$] (**2**), or [RhCp*Pf$_2$(NCMe)] (**3**), respectively (Scheme 1).[8] The acetonitrile ligand in **3** can be removed by prolonged heating in vacuum at 80 °C to produce [RhCp*Pf$_2$] (**4**)

quantitatively. The analogue of **3** with Ar = Rf can be observed in solutions of **2** and MeCN at low temperature, but fully releases the acetonitrile upon crystallization at room temperature.
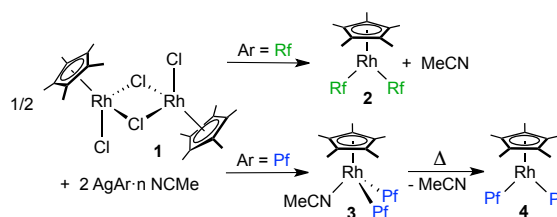
Scheme 1. Reaction of (μ-Cl)$_2$[RhCp*Cl]$_2$ with AgAr·n(NCMe).

The X-ray diffraction structures of **3** and **4** are shown in Figure 1 and that of **2** is given as supplementary information (Figure ESI1). Complex **3** shows the typical piano-stool structure of Cp-octahedral complexes. It is formally 18e, and displays a yellow colour. In contrast, complexes **2** and **4** show deep red colour in solution (almost black in crystals) corresponding to an absorption band at 505 or 513 nm (molar extinction coefficient 780 M^{-1} cm^{-1} in both cases) for **2** or **4**, respectively announcing their marked structural difference with **3**. In fact, **2** and **4** are formally 16e 5-coordinate complexes. Moreover, the missing 6th ligand does not define a vacant octahedral position, and the C$_{ipso}$–Rh–C$_{ipso}$ plane is symmetrically arranged perpendicular to the Cp* plane Very few 5-coordinate RhCp* complexes have been reported.[2,9] Their properties are interesting because they are observable models for the reactivity of the octahedral complexes, once the initial ligand dissociation has occurred.
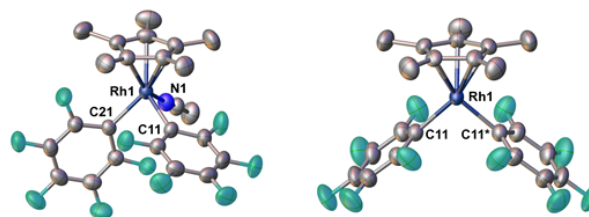
Fig. 1 X-ray structures of: Left [RhCp*Pf$_2$(NCMe)] (**3**); Right [RhCp*Pf$_2$] (**4**).

a. IU CINQUIMA/Química Inorgánica, Facultad de Ciencias, Universidad de Valladolid, 47071-Valladolid, Spain.
b. School of Chemistry, Trinity College Dublin, College Green, Dublin 2, Ireland

The weak potential acidity of the 5-coordinate complexes **2** and **4** is expressed in the formation of **3** from **4** and MeCN, a coordination equilibrium less favourable for **2** than for **4**, implying that both are slightly acidic but **4** is a better Lewis acid than **2** due to the higher electronegativity of C_6F_5 than $C_6F_3Cl_2$. This acidity order was confirmed by density functional theory (DFT) calculations, which showed a relatively high LUMO energy for **2** and **4**, with the latter being ca. 1 kcal mol^{-1} lower, as expected from its experimental higher acidity (for computational details, see ESI).

The ^{19}F NMR spectra of **2** or **4** display, in each case, chemical equivalence of the two F_{para} atoms, and of the four F_{ortho} nuclei (for **4** also the four F_{meta}). Fast Cp* rotation in solution is enough to make the five Me groups chemically equivalent and to convert into symmetry planes (on the NMR timescale) the C_{Ar}–Rh–C_{Ar} plane and the one perpendicular to it that bisects the C_{Ar}–Rh–C_{Ar} angle, producing the observed chemical equivalences.

A most interesting dynamic process operating on these systems, slower than the Cp* fluxionality just discussed, is the transmetalation exchange of Ar groups. This exchange goes unnoticed in the individual spectra of **2** or **4**, since it does not produce any observable change in their spectra. However, it becomes evident in mixtures of **2** and **4**, where the Pf/Rf labelling reveals formation of a mixed complex [RhCp*PfRf] (**5**) (Figure 2). The transmetalation equilibrium is slow enough to keep the ^{103}Rh–^{19}F coupling observable in the NMR spectra, but fast enough to produce concentrations close to equilibrium in about 1 hour at room temperature. Since the thermodynamic stability of the three complexes is very similar, the equilibrium for Scheme 2 is fairly even and the product concentrations are close to the statistical values (**2**:**4**:**5** = 1:1:2 for a 1:1 mixture of **2** and **4**).
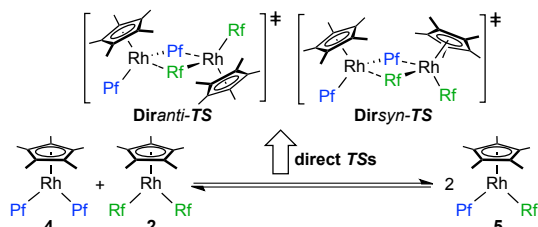
Scheme 2. Transmetalation exchange equilibrium in [RhCp*Ar$_2$] complexes, and ***non-operative*** transition states proposed for the direct mechanism (*vide infra*).

The experimental activation parameters for this transmetalation, in CDCl$_3$, were determined from the Eyring plot of the initial rates obtained by ^{19}F monitoring (Figure 2; experimental details of are given in ESI), which afforded $\Delta H^{\ddagger}_{exp}$ = 13.9±XXXX kcal mol^{-1}; $\Delta S^{\ddagger}_{exp}$ = -20±XXXX cal mol^{-1} K^{-1}; $\Delta G^{\ddagger}_{exp}$ (271 K) = 19.3±XXXX kcal mol^{-1} in the conditions measured.

The spectrum in Figure 2 uncovers also an additional unexpected fluxionality in **5** that was not apparent in **2** or in **4**: the aryl groups in all these 5-coordinate complexes are freely rotating around the Rh-C_{Ar} bond. Otherwise the spin-system of the four F_{ortho} nuclei in **5** should have a magnetically non-equivalent *through-space* coupling connection of the atom pairs involving two different *through-space* coupling constants (an AA'XX'M spin system for the $^{19}F_{ortho}$ nuclei; M stands for ^{103}Rh),

and should yield a more complex signal. The simple doublet of triplets observed is as expected for an A$_2$X$_2$M system, which proves fast Pf and Rf full rotation, since only this can give rise to the magnetic equivalence observed in the spectrum.[10]
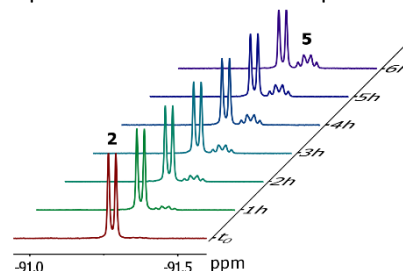
Fig. 2 F_{ortho} signals of the Rf groups of **2** (d, J$_{F-Rh}$ = 9.6 Hz) and **5** (dt, J$_{F-Rh}$ ≈ ^{ts}J$_{F-F}$ ≈ 9 Hz) showing the formation of **5** from **2** + **4** (F$_{ortho}$ signals of **4** are not shown). XXXX MHz for ^{19}F, CH$_2$Cl$_2$, at XXXK).

It is somehow unexpected that full rotation is fast in these Rh complexes with C_{Ar}–Rh–C_{Ar} angles about 95°, while in cis-PdAr$_2$ complexes, with angles close to 90°, tilting of the Pf or Rf aryl groups around the M–C_{ipso} bond is allowed, but complete free rotation is precluded.[10] This suggests that, compared to square-planar Pd^{II} complexes, the LUMO in **2**, **4**, and **5** might make more accessible the structural deformations required for the observed rotation (opening of the Ar–Rh–Ar angle).

Compared to octahedral complexes, where any transmetalation reaction would depend on prior ligand dissociation, these 5-coordinate complexes seemed to offer a privileged occasion for direct transmetalation via an uncomplicated mechanistic pathway, depicted in Scheme 2. However, very unexpectedly, DFT calculations[11] for the two possible direct transition states (**Dir***anti* or **Dir***syn*, see molecular structures in Figure ESI9) absolutely discarded this direct mechanism: the values of $\Delta G^{\ddagger}_{\text{Dir}anti}$ (39.5 kcal mol^{-1}) and $\Delta G^{\ddagger}_{\text{Dir}syn}$ (43.0 kcal mol^{-1}) in CHCl$_3$ at 271 K are too far from *pseudo*-$\Delta G^{\ddagger}_{exp}$, and too high in energy for this mechanism to have significant participation at room temperature.

The high energy of the transmetalation states of this frustrated direct exchange is a consequence of an unfortunate combination of low electrophilicity of the empty orbital in Rh with low nucleophilicity towards a second metal center of the *ipso* carbon of the fluorinated aryls that are bridging the dimer in the transition state. More important, since the mechanism assumed for the Ar exchange proves not to be correct, the experimental parameters determined from kinetics assuming direct exchange with order 1 in [**2**] and [**4**] are just *apparent* values. Thus, the deceptive apparent barrier is a *pseudo*-$\Delta G^{\ddagger}_{exp}$(271 K) value.

The fast aryl exchange observed requires the presence of some undetected highly active molecule acting as catalyst. Careful examination of the solutions of **2** (using a *cold probe* in a 500 MHz apparatus for signal to noise enhancement) detected the presence of a minute amount (less than 0.3 mol %) of *syn*-(μ-OH)$_2$[RhCp*Rf]$_2$ (**6**). This dimeric hydroxo complex is formed in variable amounts by hydrolysis of **2** in the syntheses of [RhCp*Rf$_2$] (**2**), as well as in some long-standing solutions of **2**, where the concomitant formation of RfH could be confirmed. Complex **6** is much less soluble in acetone than **2** and can be

easily separated and crystallized. An X-ray diffraction study afforded the *syn* structure of **6** shown in Figure 4, while NMR studies uncovered also the presence of its *anti* isomer (*ca*. 12%). Similarly, *syn*-(μ-OH)$_2$[RhCp*Pf]$_2$ (**7**) is formed in solutions of **4** and its structure is given in Figure ESI2. Compared to the corresponding *anti* dimers, the *syn* dimers **6** and **7** are further stabilized by the π-π stacking interactions shown in Figure 3, rendering them far more abundant in solution.[12]
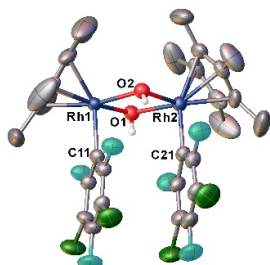

Fig. 3 X-ray structure of *syn*-(μ-OH)$_2$[RhCp*Rf]$_2$ (**6**).

The catalytic activity of **6** towards Ar exchange was experimentally confirmed by on purpose addition of **6** (5 mol %) to the reaction mixture, which accelerated the reaction about 200% (see Figure ESI4). In contrast, the other potential contaminant, complex **1**, did not catalyse the aryl exchanges. Hence we assume that the catalysis is initiated by an unobservable 16e monomer [RhCp*Rf(OH)] (**8**) formed by dissociation of **6** (*syn* or *anti*). Because the monomeric complex **8** contains a highly nucleophilic OH group, it provides a lower energy transition state for Ar exchange than the direct transmetalation in Scheme 2. Indeed, the calculated Gibbs energy profile in Figure 4 confirms the expected much lower activation energy for this exchange: $\Delta G^{\ddagger}_{\textbf{OH}anti\textbf{-}TS1}$ = 10.7 kcal mol^{-1} (CHCl$_3$, 271 K).
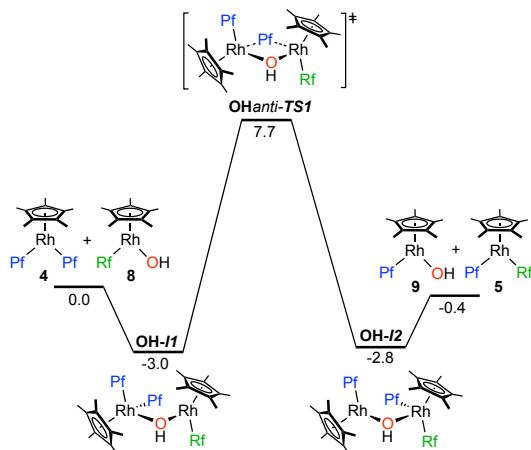

Fig. 4 Gibbs energy profile (kcal mol^{-1}, CHCl$_3$, 271K) for the **OH***anti* exchange.

Simple mathematics using $\Delta G^{\ddagger}_{\textbf{Dir}\textbf{Anti}}$ = 39.5 kcal mol^{-1} for the direct Rf/Pf transmetalation, and $\Delta G^{\ddagger}_{antiTS1}$ = 10.7 kcal mol^{-1} for the catalysed Pf/OH exchange allows to calculate that the presence of an unobservable concentration (1.2 10^{-5} mol%, in keeping with calculated K$_{dissociation}$, see ESI) of **8** or [RhCp*Pf(OH)] (**9**) in the sample of **2** or **4** is enough to reproduce the deceptive experimental value *pseudo*-$\Delta G^{\ddagger}_{exp}$ (271 K) = 19.3 kcal mol^{-1}.

In contrast to complexes **6** and **7**, where the OH group is not involved in hydrogen bonding, the calculated structures of **OH***I1*, **OH***anti-TS1*, and **OH***I2* show O–H···F–C hydrogen bond to one F$_{ortho}$ of the Pf group that is not being exchanged (see Figure ESI10). This kind of hydrogen bond is, expectedly, relatively weak. We have estimated that its contribution to the stabilization of **OH***I1* (difference for **OH***I1* Gibbs energies between two minima, one with and the other without hydrogen bonding) is about 5 kcal mol^{-1}, which matches very well other literature values.[13]

The exchange step just discussed transforms **4** into **5** using **8** (Scheme 3) and produces the new hydroxo monomer **9** (which can also be formed by dissociation of the Pf dimer **7**). Obviously, **9** can similarly transform **2** into **5** and regenerate **8** through a transition state, **OH***anti-TS2*, similar to **OH***anti-TS1* (Fig. ESI11). In other words, it is this way that the exchange process becomes catalytic, as shown in Scheme 3. The activation energies $\Delta G^{\ddagger}_{\textbf{OH}anti}$ for the cycle in Scheme 3 running clockwise are, respectively, 10.7 kcal mol^{-1} for **OH***anti-TS1* and 7.8 kcal mol^{-1} for **OH***anti-TS2*. If the cycle is taken anticlockwise, these values are 10.5 and 8.6 kcal mol^{-1}, for **OH***anti-TS1* and **OH***anti-TS2* respectively.

Scheme 3 [RhCp*Ar(OH)] catalyzed aryl exchange in [RhCp*Ar$_2$] (only productive exchanges are shown). Activation barriers for the reverse reactions are in the text.

Thus, the Rf/Pf scrambling proceeds in a catalytic way via successive Ar/OH exchanges with **8** or **9**. All activation energies are in a narrow energy range confirming the chemical similarity of the groups Rf and Pf towards transmetalation exchanges, whether productive/observable (yielding **5** from **2** and **4**) or unproductive/unobservable (yielding **2** or **4**). DFT calculations show also that the $\Delta G^{\ddagger}_{\textbf{OH}syn}$ transmetalation barriers for exchanges via **OH***syn* transition states are only slightly higher in energy than the corresponding $\Delta G^{\ddagger}_{\textbf{OH}anti}$ values. For instance, $\Delta G^{\ddagger}_{\textbf{OH}syn-TS1}$ (Figure ESI12) is 0.7 kcal mol^{-1} higher than $\Delta G^{\ddagger}_{\textbf{OH}anti-TS1}$.

The remarkable catalytic efficiency of the hydroxo monomer **8** and **9** for aryl exchanges ($\Delta G^{\ddagger}_{anti\textbf{-OH}}$ in the range 10.7–7.8 kcal mol^{-1}) as compared to the direct one ($\Delta G^{\ddagger}_{\textbf{Dir}anti}$ = 39.5 kcal mol^{-1}
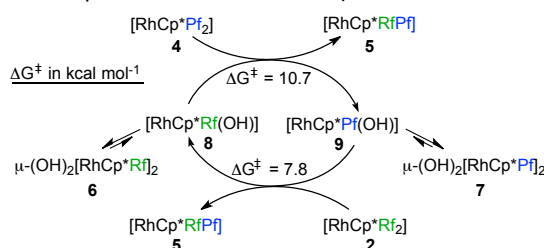
^{1}) is better understood comparing the structural features of the corresponding transition states **Dir***anti-TS* and **OH***anti-TS1* (Figure 5). The Rh–C$_{ipso}$ bond distances to the bridging aryl groups are very similar in both structures (in the range 2.238–2.443 Å) and typical of bridging 3c2e deficient bonds. It is the other side of the double bridge that makes the difference. In **Dir***anti-TS* one of the Rh–C$_{ipso}$ bond distances of the Rf group to be transmetalated is 2.163 Å (only 0.09 Å longer than the Rh–C$_{ipso}$ length of the spectator aryls: 2.082 and 2.064 Å), whereas the other one is very long (2.71 Å). These hugely different

distances, along with the orientation of its aryl plane almost in line with the Rh–C_{ipso} bond, suggest that the bridging participation of the second aryl is modest and contributes only slightly to stabilize the transition state. In contrast, the bridging OH group in **OH*anti*-TS1** is extremely efficient and makes two short bond distances (2.083 and 2.095 Å) indicating covalent 2c2e O-Rh bonds.[14] The commented difference in stability of the two transition states is well reflected in the proximity of the two Rh atoms in **OH*anti*-TS1** (distance Rh···Rh = 3.334 Å), compared to **Dir*anti*-TS** (distance Rh···Rh = 3.585 Å), as a consequence of the strength of the OH bridge. However, natural bond (NBO) analysis shows no significant Rh–Rh bonding interaction in any of the structures.
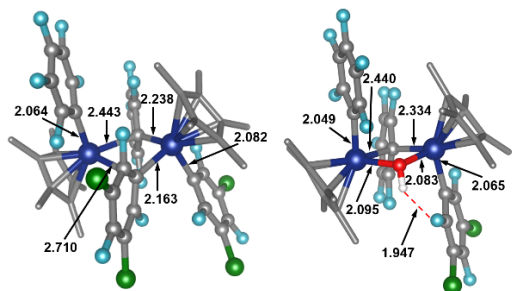

Fig. 5 Calculated transition states **Dir*anti*** (left) and **OH*anti*-TS1** (right). Relevant bond distances (Å) are shown.

In summary, stable five-coordinate 16e [RhCp*Ar$_2$] (Ar = Pf, Rf) complexes reveal some chemical phenomena that can operate on 18e Rh(III) complexes after initial ligand dissociation. The mismatch between DFT calculations and experimental data questions the apparently obvious mechanistic proposal for aryl exchange in these 16e mononuclear complexes. Experimental re-examination reveals that this exchange is catalysed by the presence, in undetectable concentration, of adventitious [RhCp*Ar(OH)] species (Scheme 3). No exchange would occur at detectable rate without these catalysts. The moral is that even apparently obvious conclusions from clear observations should better be supported by additional data and DFT calculations.

The extraordinarily stabilizing effect found for the participation of OH in bridged structures, compared to the more modest effect of Cl in bridges, is a relevant finding with potential practical application to transmetalations in other chemical systems.

It is worth recalling that similar hydroxo- and oxo-bridged dimers may be involved in Ir-catalysed water oxidation processes.[3, 15-17] Research on related Ir^{III} complexes is ongoing.

Notes and references

1   M. García-Melchor, A. A. C. Braga, A. Lledós, G. Ujaque and F. Maseras, *Acc. Chem. Res.,* 2013, **46**, 2626.

2   Q. Wu, Y. Chen, M. Yan, Y. Lu, W.-Y. Sun and J. Zhao, *Chem. Sci.*, 2017, **8**, 169.

3   (a) J. D. Blakemore, R. H. Crabtree and G. W. Brudvig, *Chem Rev.* 2015, **115**, 12974. (b) J. D. Blakemore, N. D. Schley, D. Balcells, J. F. Hull, G. W. Olack, C. D. Incarvito, O. Eisenstein, G. W. Brudvig and R. H. Crabtree, *J. Am. Chem. Soc.,* 2010, **132**, 16017. (c) J. Graeupner, T. P. Brewster, J. D. Blakemore, N. D. Schley, J. M. Thomsen, G. W. Brudvig, N. Hazari, R. H. Crabtree, *Organometallics,* 2012, **31**, 7158.

4   RhCp* complexes were first prepared from hexamethyl Dewar benzene by a reaction involving ring contraction, and some years later from Cp*H: (a) J. W. Kang, K. Mosley and P. M. Maitlis, *Chem. Commun.*, 1968, **21**, 1303. (b) J. W. Kang and P. M. Maitlis, *J. Am. Chem. Soc.,* 1968, **90**, 3259. (c) J. W. Kang and P. M. Maitlis, *J. Am. Chem. Soc.,* 1969, **91**, 5970. (d) C. White, A. Yates, P. M. Maitlis and D. M. Heinekey, *Inorg. Synth.,* 1992, **29**, 228.

5   The best recent preparation of RhCp* complexes uses Cp*H and microwave heating: J. Tönnemann, J. Risse, Z. Grote, R. Scopelliti and K. Severin, *Eur. J. Inorg. Chem*. 2013, 4558.

6   These silver reagents are precipitated from their acetonitrile solutions. Only AgPf was reported. We have used the same procedure for AgRf: (a) K. K. Sun and W. T. Miller, *J. Am. Chem. Soc.*, 1970, **92**, 6985. The presence of acetonitrile was confirmed by X-ray diffraction: (b) M. Kuprat, M. Lehmann, A. Schulz and A. Villinger, *Organometallics*, 2010, **29**, 1421.

7   AgPf and [Ag(Pf)$_2$]$^-$ have been used to obtain Rh^{III} or Rh^{I} compounds: (a) M. P. García, M. V. Jiménez, F. J. Lahoz and L. A. Oro, *Inorg. Chem.*, 1995, **34**, 2153. (b) R. L. Bennett, M. I. Bruce and R. C. F. Gardner, *J. C. S. Dalton Trans.,* 1973, 2653.

8   For RhCp* 5-coordinate complexes, see ref. 2, and: (a) P. Espinet, P. M. Bailey and P. M. Maitlis, *J. Chem. Soc., Dalton Trans.* 1979, 1542. (b) M. Sakamoto, Y. Ohki and K. Tatsumi, *Organometallics,* 2010, **29**, 1761.

9   For Au/Rh transmetalation in catalysis see: Y. Shi and S. A. Blum, *Organometallics,* 2011, **30**, 1776.

10 For spectral analysis in systems with fluorinated aryls connected by *through-space* ^{19}F–^{19}F coupling see: P. Espinet, A. C. Albéniz, J. A. Casares and J. M. Martínez-Ilarduya, *Coord. Chem. Rev.*, 2008, **252**, 2180.

11 Using the dispersion corrected hybrid functional ωB97X-D: J.-D. Chai and M. Head-Gordon, *Phys. Chem. Chem. Phys.,* 2008, **10**, 6615.

12 The dimer in the solid state of (μ-OH)Rh^{III}Cp* systems is *anti* (ref. 12a), unless π-π stacking stabilizes the *syn* dimer (ref. 12b): (a) L. A. Oro, D. Carmona, M. P. Lamata, M. C. Apreda, C. Foces-Foces, F. H. Cano and P. M. Maitlis, *J. Chem. Soc., Dalton Trans.,* 1984, 1823. (b) R. H. Fish, H.-S. Kim, J. E. Babin and R. D. Adams, *Organometallics,* 1988, **7**, 2250.

13 (a) C. Bartolomé, P. Espinet and J. M. Martin-Álvarez, *Chem. Commun.,* 2007, 4384. (b) C. Bartolomé, F. Villafañe, J. M. Martín-Alvarez, J. M. Martínez-Ilarduya and P. Espinet, *Chem. Eur. J.,* 2013, **19**, 3702.

14 B. Cordero, V. Gómez, A. E. Platero-Prats, M. Revés, J. Echeverría, E. Cremades, F. Barragán and S. Álvarez, *Dalton Trans.,* 2008, 2832.

15 R. J. Burford, W. E. Piers, D. H. Ess and M. Parvez, *J. Am. Chem. Soc.,* 2014, **136**, 3256.

16 L. S. Sharninghausen, S. B. Sinha, D. Y. Shopov, B. Choi, B. Q. Mercado, X. Roy, D. Balcells, G. W. Brudvig and R. H. Crabtree, *J. Am. Chem. Soc.,* 2016, **138**, 15917.

17 M. García-Melchor, L. Vilella, N. López and A. Vojvodic, *ChemCatChem,* 2016, **8**, 1792.